Journal of Photochemistry and Photobiology A: Chemistry 294 (2014) 54–61

Contents lists available at ScienceDirect

Journal of Photochemistry and Photobiology A: Chemistry

journal homepage: www.elsevier.com/locate/jphotochem

New D–π-A system dye based on dithienosilole and carbazole: Synthesis, photo-electrochemical properties and dye-sensitized solar cell performance

Jie Liu[a], Xiang Sun[a], Zhifang Li[b], Bin Jin[a], Guoqiao Lai[b], Haiying Li[c], Chengyun Wang[a,*], Yongjia Shen[a], Jianli Hua[a]

[a] Key Laboratory for Advanced Materials and Institute of Fine Chemicals, East China University of Science and Technology, 130 Meilong Road, Shanghai, 200237, China
[b] Key Laboratory of Organosilicon Chemistry and Material Technology of Ministry of Education, Hangzhou Normal University, Hangzhou 310012, China
[c] Key Laboratory for Advanced Materials and Department of Chemistry, East China University of Science and Technology, 130 Meilong Road, Shanghai, 200237, China

ARTICLE INFO

Article history:
Received 8 April 2014
Received in revised form 24 June 2014
Accepted 24 July 2014
Available online 2 August 2014

Keywords:
Carbazole
Dithienosilole
π-Conjugated system
Power conversion efficiency
Dye-sensitized solar cell

ABSTRACT

New donor–linker–acceptor pattern organic dye containing a dithienosilole unit as a π-conjugated system, a carbazole moiety as an electron donor, and a cyanoacrylic acid unit as an electron acceptor was synthesized for application in dye-sensitized solar cell (**DSSC**). Its photophysical and electrochemical properties were investigated, the dithienosilole unit could dramatically lower the lowest unoccupied molecular orbital (**LUMO**) level and energy gap. Its performances as sensitizers in solar cells were measured, and possessed a power conversion efficiency of 4.80%.

1. Introduction

Photovoltaic cell is of great significance in energy territory for its clean and recyclable characteristics. Although inorganic solar cell still currently dominates the photovoltaic field, it is greatly limited by either costly or hazardous materials involved in the technologies. In contrast, dye-sensitized solar cell (**DSSC**) draws many attentions for its low-cost, versatile, energy-saving, and environmental friendly performance.

Dye sensitizer is the key part of **DSSC**. Generally speaking, sensitizer in high performance should have wide and strong absorption in the visible region, good solubility, appropriate lowest unoccupied molecular orbital (**LUMO**) and highest occupied molecular orbital (**HUMO)** level for effective electron-injection to the semiconductor's conduction band and dye regeneration [1]. Recently, researched interesting has been focused on the Donor–π-Acceptor (**D–π-A**) system owing to its effective photo-induced intra-molecular charge-transfer characteristics [2]. Wang and co-workers reported a sensitizer C219 with dihexyl-substituted dithienosilole and 3,4-ethylenedioxythiophene unit as the binary π-conjugated spacer between alkoxy-substituted triphenylamine electron donor and cyanoacrylic acid electron acceptor, exhibiting promising photovoltaic property [3].

Arylamine-based moieties are employed as the electron donor (**D**) frequently for their strong electron-donating nature [4]. As arylamine derivative, carbazole shares its strong electron-giving capacity and has been studied for different applications [5,6]. Castellano and co-workers synthesized carbazole or bithiophene bridged sensitizers and obtained a conversion efficiency of 2.70% [7]. Koumura and co-workers researched on a series of sensitizers with carbazole as the **D** unit, repeating thiophenes as the π moiety and cyanoacrylate as the electron-drawing part, and the **DSSC** reached a high power conversion efficiency [8,9]. Li and co-workers researched indole-based carbazole and got a conversion efficiency of 4.31%, and a pyrrole-containing carbazole with a conversion efficiency of 4.62% [10]. Roncali and co-workers researched similar substituted triarylamine donors and got a conversion efficiency of 1.92% [11]. These reports encouraged us to explore the application of carbazole as the electron donor for the **D–π-A** pattern dye. Besides, carbazole has good thermo and

* Corresponding author. Tel.: +86 021 64252967; fax: +86 021 64252967.
E-mail address: cywang@ecust.edu.cn (C. Wang).

http://dx.doi.org/10.1016/j.jphotochem.2014.07.021
1010-6030/

chemical stability, which is favorable for the long lifetime of **DSSC**.

In this paper, we reported the design, synthesis and properties of a new dye sensitizer in D–π-A pattern. A binary π moiety comprising thiophene and 4,4-dioctyl dithienosilole (**DODTS**) was employed in the system. Thiophene and DODTS are linked by ethynyl, which can broaden the π-conjugation of the dye molecule. The synthesis, properties and applications of siloles have been widely studied for many years [12]. As a derivative of silole, **DODTS** shows low **LUMO** energy level characteristic and has good coplanarity as well as electron-transfer capacity [13,14]. So the incorporation of **DODTS** as one of the binary π moieties will facilitate the electron-transfer process and lower the **LUMO** level of the dye. Carbazole is used as the **D** unit for its outstanding electron-donating ability and thermo stability. Cyanoacrylic acid works as the electron acceptor. Its strong electron-drawing ability contributes to the intra-molecular charge transfer, and carboxyl helps the dye to adsorb on the TiO_2 particles. Therefore, it may have promising prospects in the field of DSSC.

2. Experimental section

2.1. Materials and measurements

Unless otherwise stated, all solvents and reagents were chemical pure or analytical pure and used as received from commercial sources without further purification. Solvents for chemical synthesis such as tetrahydrofuran (THF), triethylamine, 1,2-dichloroethane were purified by dehydration and distilled with standard methods. Lithium diisopropylamide (LDA) was prepared [15] and used soon after its preparation. $Pd(PPh_3)_2Cl_2$ was synthesized according to Ref. [16] and stored in dry container. The nuclear magnetic resonance (NMR) spectra were obtained from a Bruker Avance III 400 (in $CDCl_3$). Mass spectra were obtained using Micromass LCTTM (HREI-TOF). The UV–vis spectra were recorded by a Varian Cary00 UV–vis Spectrometer (THF as solvent). Fluorescence spectra were recorded by a Varian Cary Eclipse Fluorescence Spectrometer (THF as solvent).

2.2. Synthetic procedures and characterizations

3,3′-Dibromo-2,2′-bithiophene (2): In a 250 mL three neck flask, 3-bromothiophene (4.0 g, 24.54 mmol) was solved in anhydrous THF (50 mL). The solution was cooled to −78 °C and LDA solution was added dropwise over 20 min. Then the solution was stirred for 1 h at the same temperature and $CuCl_2$ (6.56 g, 49.08 mmol) was added in one portion. After being stirred for 1 h at −78 °C, the mixture was warmed to room temperature and stirred for another 5 h. The reaction was quenched with water. The crude compound was extracted with dichloromethane and washed by distilled water, dried over anhydrous $MgSO_4$, and evaporated in vacuum. The residue was purified by silica gel column chromatography (eluent: petroleum ether). Compound **2** was obtained as a white solid (1.7 g, 42%). ^{1}H NMR ($CDCl_3$, 400 MHz): δ 7.41 (d, J = 5.4 Hz, 2*H*, SCH), 7.08 (d, J = 5.4 Hz, 2*H*, SCCH).

LDA solution was prepared with *n*-BuLi and diisopropylamine by following method [15]: Diisopropylamine (3.0 g, 29.45 mmol) was solved in THF (10 mL), and cooled to −78 °C, then *n*-BuLi (1.6 M solution, 19 mL) was added and stirred for 1 h, therefore LDA solution was obtained and used soon after its preparation.

4,4-Dioctyl-dithieno[3,2-b:2′,3′-d]silole (3): A mixture of 1.6 M *n*-BuLi in hexane (3.7 mL, 5.92 mmol), anhydrous THF (40 mL) in a round-bottom flask was cooled to −78 °C, then a solution of **2** (800 mg, 2.47 mmol) in anhydrous THF (10 mL) was added dropwise over 15 min under vigorous stirring. After being stirred for 1 h at −78 °C, the solution resulted in a white suspension. Then a solution of dichlorodioctylsilane (963 mg, 2.96 mmol) in THF (10 mL) was added dropwise. The mixture was stirred for another 5 h at −78 °C, warmed to room temperature, and stirred overnight. The reaction was quenched by saturated aqueous NH_4Cl solution (30 mL).The aqueous layer was extracted with dichloromethane (3 × 15 mL). The combined organic layers were washed with water, dried over anhydrous $MgSO_4$, filtrated, evaporated in vacuum to remove the solvent. Then the crude product was purified by column chromatography with petroleum ether as eluent to yield a light green oil (210 mg, 20%). ^{1}H NMR ($CDCl_3$, 400 MHz): δ 7.18 (d, J = 4.7 Hz, 2*H*, SCH), 7.04 (d, J = 4.7 Hz, 2*H*, SCCH), 1.40–1.19 (m, 24*H*), 0.92–0.82 (m, 10*H*).

4,4-Dioctyl-dithieno[3,2-b:2′,3′-d]silole-2-carbaldehyde (4): To a stirring solution of **3** (300 mg, 0.72 mmol) and *N*,*N*-dimethylformamide (63 mg, 0.86 mmol) in dry 1,2-dichloroethane (20 mL) was added dropwise phosphorus-oxychloride (442 mg, 2.88 mmol) at 0 °C. The reaction mixture was then heated to 70 °C and stirred for 4 h. After being cooled to room temperature, the reaction mixture was quenched with saturated sodium acetate aqueous solution (20 mL) and extracted with ethyl acetate (15 × 3 mL). The combined organic layers were washed with brine, dried over anhydrous magnesium sulfate, filtered and evaporated in vacuum to remove the solvent. The crude product was purified by column chromatography on silica gel with dichloromethane/petroleum ether (v/v, 1:1) as eluent to afford **4** as a yellow oil (259 mg, 81%). ^{1}H NMR ($CDCl_3$, 400 MHz): δ 9.86 (s, 1*H*, CHO), 7.71 (s, 1*H*, SCCH), 7.39 (d, J = 4.7 Hz, 1*H*, SCH), 7.12 (d, J = 4.7 Hz, 1*H*, SCCH), 1.39–1.21 (m, 24*H*), 0.89–0.84 (m, 10*H*).

4,4-Dioctyl-6-bromo-dithieno[3,2-b:2′,3′-d]silole-2-carbaldehyde (5): To a stirring solution of **4** (200 mg, 0.45 mmol) in chloroform (25 mL) was added dropwise *N*-bromosuccinimide (96 mg, 0.54 mmol)) in dichloromethane (10 mL) at 0 °C. The reaction mixture was then warmed to room temperature and stirred for 12 h. The mixture was poured into water and extracted with diethyl ether. The combined extracts were washed with brine, dried over anhydrous sodium sulfate, filtered, and evaporated in vacuum to remove the solvent. The crude product was purified by a short silica gel column with dichloromethane/petroleum ether (v/v, 1:1) as eluent to afford **5** as a yellow solid (212 mg, 90%). ^{1}H NMR ($CDCl_3$, 400 MHz): δ 9.87 (s, 1*H*, CHO), 7.70 (s, 1*H*, SCCH), 7.08 (s, 1*H*, SCBrCH), 1.41–1.21 (m, 24*H*), 0.94–0.85 (m, 10*H*).

9-(Thiophen-2-yl)-9*H*-carbazole (7): A mixture of CuI (0.68 g, 3.6 mmol), 18-Crown-6 (0.48 g, 1.8 mmol), K_2CO_3 (8.3 g, 60 mmol), carbazole (6.00 g, 35.88 mmol), 2-bromothiophene (5.85 g, 35.88 mmol) and *N*,*N*-dimethyl formamide (DMF) (100 mL) was heated at 170 °C for 24 h under nitrogen. After cooling to room temperature, the mixture was quenched with 1 M HCl solution. The Precipitate was filtered and washed with $NH_3{\cdot}H_2O$ and water. The gray crude product was purified by a short silica gel column with dichloromethane/petroleum ether (v/v, 1:10) as eluent to afford **7** as a light yellow solid (2.77 g, 31%). ^{1}H NMR ($CDCl_3$, 400 MHz): δ 8.12 (d, J = 7.8 Hz, 2*H*, $C_{12}H_8N$), 7.49–7.45 (m, 4*H*, $C_{12}H_8N$), 7.41–7.38 (d, J = 4.0 Hz, 1*H*, SCH), 7.35–7.30 (m, 2*H*, $C_{12}H_8N$), 7.22–7.19 (m, 2*H*, SCCH).

9-(5-Bromothiophen-2-yl)-9*H*-carbazole (8): To a stirring solution of **7** (800 mg, 3.21 mmol) in dichloromethane (50 mL) was dropwise added *N*-bromosuccinimide (685 mg, 3.85 mmol) in dichloromethane/acetic acid (25/25 mL) at 0 °C. The reaction mixture was then warmed to room temperature and stirred for 12 h. The mixture was poured into water and extracted with diethyl ether. The combined extracts were washed with brine, dried over anhydrous sodium sulfate, filtered, and evaporated in vacuum to remove the solvent. The crude product was purified by a short silica gel column with dichloromethane/petroleum ether (v/v, 1:1) as eluent to afford **8** as a yellow solid (948 mg, 90%). ^{1}H NMR (400 MHz,

$CDCl_3$): δ 8.09 (d, *J* = 7.8 Hz, 2*H*, $C_{12}H_8N$), 7.45–7.42 (m, 4*H*, $C_{12}H_8N$), 7.33–7.28 (m, 2*H*, $C_{12}H_8N$), 7.16 (d, *J* = 3.9 Hz, 1*H*, SCCH), 6.98 (d, *J* = 3.9 Hz, 1*H*, SCCH).

4-(5-(9*H*-carbazol-9-yl)thiophen-2-yl)-2-methylbut-3-yn-2-ol (9): To a stirring solution of compound **8** (900 mg, 2.74 mmol) in triethylamine (60 mL) were added $Pd(PPh_3)_2Cl_2$ (96 mg, 0.14 mmol), PPh_3 (72 mg, 0.27 mmol), CuI (52 mg, 0.27 mmol) under Argon. Then 2-methyl-3-butyn-2-ol (690 mg, 8.22 mmol) was added dropwise to the stirring mixture. The reaction mixture was stirred at room temperature for 6 h. The solvent was removed by evaporating in vacuum. The crude product was purified by a short silica gel column with dichloromethane/petroleum ether (v/v, 1:2) as eluent to afford **9** as an orange oil (745 mg, 82%). ^{1}H NMR (400 MHz, $CDCl_3$): δ 8.06 (d, *J* = 7.7 Hz, 2*H*, $C_{12}H_8N$), 7.48–7.38 (m, 4*H*, $C_{12}H_8N$), 7.30–7.26 (m, 2*H*, $C_{12}H_8N$), 7.21 (d, *J* = 3.9 Hz, 1*H*, SCCH), 7.02 (d, *J* = 3.9 Hz, 1*H*, SCCH), 1.63 (s, 6*H*, $2CH_3$).

9-(5-Ethynylthiophen-2-yl)-9*H*-carbazole (10): A mixture of compound **9** (400 mg, 1.21 mmol), potassium hydroxide (135 mg, 2.42 mmol) in isopropanol was heated to 70 °C under argon atmosphere. After being stirred for 8 h at 70 °C, the reaction mixture was added by water and extracted by dichloromethane. The combined extracts were washed with brine, dried over anhydrous sodium sulfate, filtered, and evaporated in vacuum to remove the solvent. The residue was purified by column chromatography on a silica gel column with petroleum/dichloromethane (v/v, 10/1) as eluent. Compound **10** was obtained as a white solid (240 mg, 73%). ^{1}H NMR (400 MHz, $CDCl_3$): δ 8.06 (d, *J* = 7.7 Hz, 2*H*, $C_{12}H_8N$), 7.52–7.42 (m, 4*H*, $C_{12}H_8N$), 7.36 (d, *J* = 3.9 Hz, 1*H*, SCCH), 7.34–7.30 (m, 2*H*, $C_{12}H_8N$), 7.08 (d, *J* = 3.9 Hz, 1*H*, SCCH), 3.40 (s, 1*H*, C≡CH).

6-(1-(2-(Carbazol-9-yl)-thiophen-5-yl)-ethynyl)-4,4-dioctyl-dithieo[3,2-b:2′,3′-d]silole-2-carbaldehyde (11): To a stirring solution of compound **5** (100 mg, 0.19 mmol) in triethylamine (30 mL) were added $Pd(PPh_3)_2Cl_2$(14 mg, 0.02 mmol), CuI (7 mg, 0.04 mmol) under Argon. Then compound **10** (104 mg, 0.38 mmol) in triethylamine (10 mL) was added dropwise to the stirring mixture. The reaction mixture was stirred for 6 h at 80 °C. The solvent was removed by evaporating in vacuum. The crude product was purified by a silica gel column with dichloromethane/petroleum ether (v/v, 1:2) as eluent to afford **11** as an orange-red oil (55 mg, 40%). ^{1}H NMR (400 MHz, $CDCl_3$): δ 9.88 (s, 1*H*, CHO), 8.11 (d, *J* = 7.7 Hz, 2*H*, $C_{12}H_8N$), 7.72 (s, 1*H*, SCCH), 7.55 (d, *J* = 8.2 Hz, 2*H*, $C_{12}H_8N$), 7.46 (dd, J_1 = 8.2 Hz, J_2 = 7.2 Hz, 2*H*, $C_{12}H_8N$), 7.35–7.30 (dd, J_1 = 7.7 Hz, J_2 = 7.2 Hz, 2*H*, $C_{12}H_8N$), 7.27 (d, *J* = 3.8 Hz, 1*H*, SCCH),7.22 (s, 1*H*, SCCH), 7.14 (d, *J* = 3.8 Hz, 1*H*, SCCH), 1.34–1.22 (m, 24*H*), 0.90–0.83 (m, 10*H*).

3-(6-(1-(2-(Carbazol-9-yl)-thiophen-5-yl)-ethynyl)-4,4-dioctyl-dithieo[3,2-b:2′,3′-d]silole-2-yl-)-2-cyanoacrylic acid (CTDTSCA): To a stirred solution of compound 11 (100 mg, 0.14 mmol) and cyanoacetic acid (48 mg, 0.56 mmol) in chloroform (30 mL) was added piperidine (0.1 mL). The reaction mixture was refluxed for 12 h and then acidified with 2 M hydrochloric acid aqueous solution (20 mL). The crude product was extracted into chloroform, washed with water, and dried over anhydrous sodium sulfate. After removing solvent under reduced pressure, the residue was purified by flash chromatography with dichloromethane and methanol/dichlormehane (v/v, 1:10) in turn as eluent to yield a red solid (77 mg, 70%). ^{1}H NMR (400 MHz, $CDCl_3$): δ 8.34 (s, 1*H*, C═CH), 8.11 (d, *J* = 7.7 Hz, 2*H*, $C_{12}H_8N$), 7.74 (s, 1*H*, SCCH), 7.55 (d, *J* = 8.2 Hz, 2*H*, $C_{12}H_8N$), 7.46 (dd, J_1 = 8.2, J_2 = 7.2, 2*H*, $C_{12}H_8N$), 7.38 (d, *J* = 3.7 Hz, 1*H*, SCCH), 7.35–7.32 (m, 3*H*, $C_{12}H_8N$ & SCCH), 7.14 (d, *J* = 3.8 Hz, 1*H*, SCCH), 1.34–1.22 (m, 24*H*), 0.90–0.82 (m, 10*H*). HRMS (ESI, *m*/*z*): $[M]^+$ calcd for $C_{46}H_{47}N_2O_2S_3Si$, 784.2647; found, 784.2579. IR (KBr, cm^{-1}): 2959, 2921, 2848, 2211, 1729, 1638, 1613, 1462, 1385, 1264, 1098, 1024, 805, 620.

3-(4,4-Dioctyl-dithieo[3,2-b:2′,3′-d]silole-2yl-)-2-cyanoacrylic acid (DTSCA): DTSCA was prepared by a Knoevenagel condensation reaction between compound **4** and cyanoacetic acid. The concrete operations were similar to the synthesis of CTDTSCA from compound **11**. ^{1}H NMR (400 MHz, $CDCl_3$): δ 8.37 (s, 1*H*, C═CH), 7.74 (s, 1*H*, SCCH), 7.46 (d, *J* = 4.5 Hz, 1*H*, SCH), 7.14 (d, *J* = 4.6 Hz, 1*H*, SCCH), 1.34–1.22 (m, 24*H*), 0.90–0.82 (m, 10*H*). HRMS (ESI, *m*/*z*): $[M]^+$ calcd for $C_{28}H_{38}NO_2S_2Si$, 513.2191; found, 513.2145. IR (KBr, cm^{-1}): 2967, 2921, 2848, 2215, 1711, 1574, 1470, 1380, 1261, 1100, 1019, 804, 709, 615.

3-(5-(9*H*-carbazol-9-yl) thiophen-2-yl)-2-cyanoacrylic acid (CTCA): CTCA was prepared through a Vilsmeier–Haack reaction and a Knoevenagel condensation reaction from compound **7**. The Vilsmeier–Haack reaction of compound **7** was similar to that of compound **3**, the Knoevenagel condensation reaction of compound **12** and cyanoacetic acid was similar to that of compound **11**. ^{1}H NMR (400 MHz, $CDCl_3$): δ 8.39 (s, 1*H*, C═CH), 8.10 (d, *J* = 7.7, 2*H*, $C_{12}H_8N$), 7.93–7.88(m, 1*H*, SCCH), 7.71–7.66 (m, 2*H*, $C_{12}H_8N$), 7.51–7.45 (m, 2*H*, $C_{12}H_8N$), 7.39–7.34 (m, 3*H*, $C_{12}H_8N$ & SCCH). HRMS (ESI, *m*/*z*): $[M]^+$ calcd for $C_{20}H_{11}N_2O_2S$, 344.0619; found, 344.0629. IR (KBr, cm^{-1}): 2924, 2850, 2200, 1621, 1519, 1394, 1077, 727.

2.3. Cyclic voltammetry

The cyclic voltammograms of the dyes adsorbed on the TiO_2 film was measured with a Versastat II electrochemical workstation (Princeton Applied Research) using 0.1 M $TBAPF_6$ (Aldrich) as the supporting electrolyte, the sensitizer attached to a nanocrystalline TiO_2 film deposited on the conducting FTO glass as the working electrode, a platinum wire as the counter electrode, and a regular calomel electrode in saturated KCl solution as the reference electrode. The scan rate was 100 mV s^{-1}.

2.4. Fabrication of dye-sensitized solar cells

A screen–printed double layer of titania particles were used as the photoelectrode. A 10 μm layer of 13 nm TiO_2 nanoparticles was first printed on the clean FTO conducting glass plates. After the film was dried at 125 °C over 6 min, another 4 μm layer of 400 nm light-scattering anatase particles was coated on. Then the electrodes were gradually sintered in a muffle furnace at 275 °C for 5 min, at 325 °C for 5 min, at 375 °C for 5 min, at 450 °C for 15 min and at 500 °C for 15 min, respectively. The size of the TiO_2 film was 0.25 cm^2. These films were immersed into a 40 mM aqueous $TiCl_4$ solution at room temperature for 12 h, then washed with water and ethanol. The films were then heated at 450 °C for 30 min. After cooling, the TiO_2 electrodes were immersed into the dye solutions of 1 mM in dichloromethane at room temperature for 12 h. Counter electrodes of the **DSSC** were prepared by spin-coating three drops of 0.02 M H_2PtCl_6 in 2-propanol on the FTO glass plates followed by annealing treatment at 400 °C for 15 min. The dye-anchored TiO_2 working electrode and the counter electrode were assembled into a sealed **DSSC** cell with a hot-melt gasket between them. A drop of electrolyte solution was injected into the cell through a drilled hole. The electrolyte solution was consisted of 0.5 M 1-butyl-3-methylimidazolium iodide (BM II), 0.1 M 1,2-dimethyl-3-propylimidazolium iodide (DMP II), 0.03 M I_2, 0.05 M LiI, 0.5 M 4-*tert*-butylpyridine (*t*BP) and 0.1 M guanidinium thiocyanate (GT) in acetonitrile-valeronitrile(85:15, v/v). Finally, the hole was sealed using a UV-melt gum and a cover glass.

2.5. Photovoltaic measurements

Photovoltaic measurements employed an AM 1.5 solar simulator equipped with a 300 W xenon lamp (model no. 91160, Oriel). The power of the simulated light was calibrated to 100 mW cm^{-2} using a Newport Oriel PV reference cell system (model 91150 V).

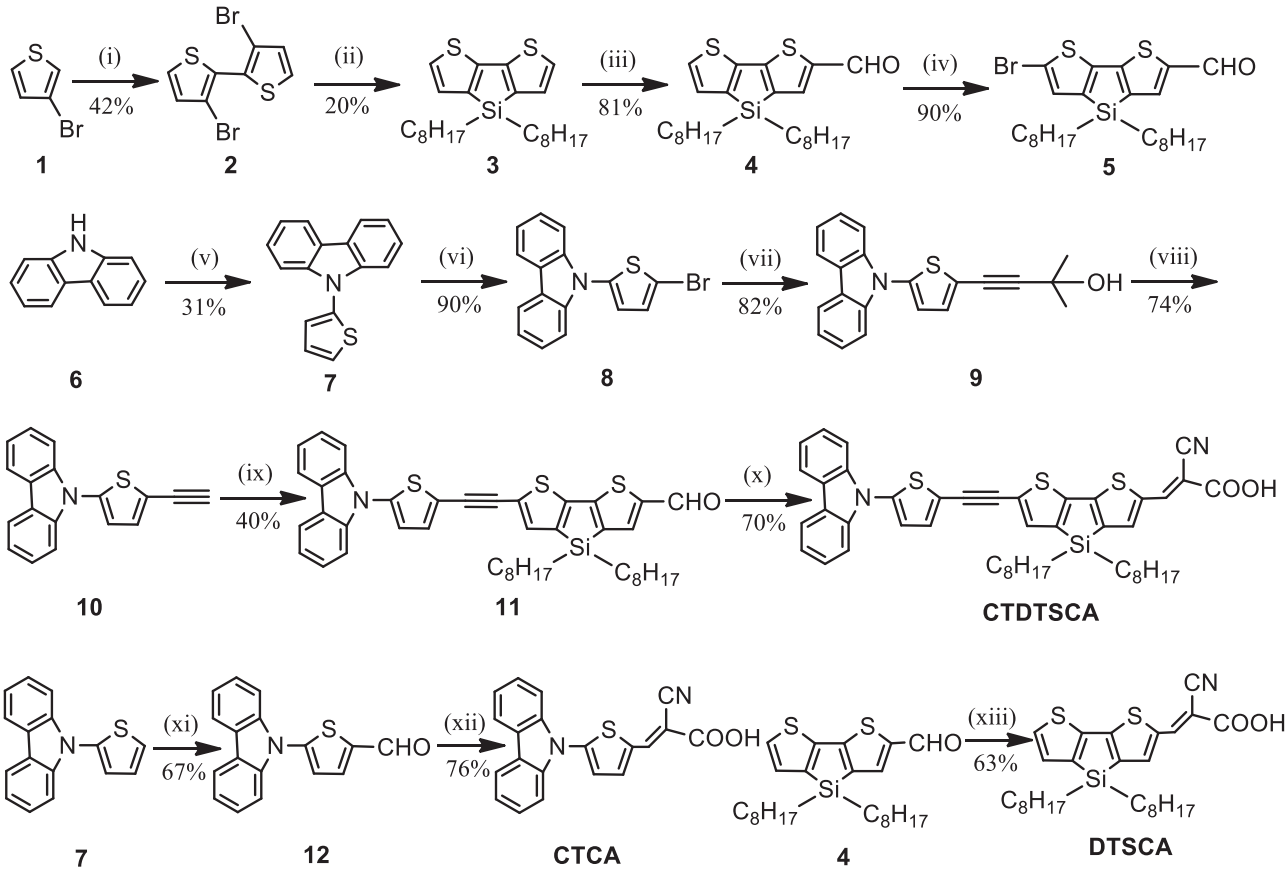

Scheme 1. Synthetic routes of **CTDTSCA**, **DTSCA** and **CTCA**. Reagents and conditions: (i) −78 °C, LDA, THF, $CuCl_2$; (ii) −78 °C, *n*BuLi, dichlorodioctylsilane; (iii) 80 °C, $POCl_3$, DMF, 1, 2-dichloroethane; (iv) rt., NBS, chloroform; (v) 170 °C, 2-bromothiophene, CuI, 18-Crown-6, K_2CO_3; (vi) rt., NBS, dichloromethane/acetic acid; (vii) rt., $Pd(PPh_3)_2Cl_2$, PPh_3, CuI, 2-methyl-3-butyn-2-ol, triethylamine; (viii) refluxed, KOH, isopropanol; (ix) 70 °C, compound **5**, $Pd(PPh_3)_2Cl_2$, PPh_3, CuI, triethylamine; (x) 70 °C, cyanoacetic acid, piperidine, chloroform; (xi) 80 °C, $POCl_3$, DMF, 1, 2-dichloroethane; (xii) 70 °C, cyanoacetic acid, piperidine, chloroform; (xiii) 70 °C, cyanoacetic acid, piperidine, chloroform.

Current density–voltage (*J–V*) curves were obtained by applying an external bias to the cell and measuring the generated photocurrent with a model 2400 source meter (Keithley Instruments Inc. USA). The voltage step and delay time of the photocurrent were 10 mV and 40 ms, respectively. Action spectra of the incident monochromatic photon-to-electron conversion efficiency (IPCE) for the solar cells were measured on a Newport-74125 system (Newport Instruments). The intensity of monochromatic light was measured with a Si detector (Newport-71640). The electrochemical impedance spectroscopy (EIS) measurements of all the DSSC were performed using a Zahner IM6e Impedance Analyzer (Zahner-Elektrik GmbH & CoKG, Kronach, Germany). The frequency range is 0.1 Hz–100 kHz. The magnitude of the alternative signal is 10 mV.

2.6. Theoretical calculations

Theoretical calculations based on density functional theory method have been performed with Gaussian 09 program [17]. The calculations were performed with the B3LYP exchange correlation functional under 6–31G (d) basis.

3. Results and discussion

3.1. Synthesis

CTDTSCA was obtained by several steps according to the synthetic routes shown in Scheme 1. Starting from the coupling of 3-bromothiophene in the presence of LDA and $CuCl_2$, [18] 4,4′-dioctyl-dithieo[3,2-b:2′,3′-d]silole (**3**) was obtained by the reaction of compound **2** and dichlorodioctylsilane [19]. Compound **4**, prepared in a high yield of 81% through selective monoformylation of **3** by controlling the dosage of DMF and $POCl_3$ [20], was brominated by *N*-bromosuccinimide (NBS) in chloroform to afford **5** [21]. Chloroform used as solvent in the bromination step avoided the inconvenience of using hard-removed DMF [22]. The electron donor unit was synthesized in several steps with carbazole and 2-bromothiophene as original materials. Carbazole and 2-bromothiophene were refluxed in a mixture of CuI, 18-Crown-6, K_2CO_3 in DMF to afford **7** in 31% yield [23]. Compound **8**, prepared by monobromination of **7**, was reacted with 2-methylbut-3-yn-2-ol under the catalysis of $Pd(PPh_3)_2Cl_2$, PPh_3, CuI in argon protection to afford **9** in 82% yield [24]. The terminal acetylene **10** was synthesized in 74% yield by refluxing of **9** in potassium hydroxide/isopropanol solution [25]. After synthesizing **11** through Sonogashira reaction of **10** and **5**, the final dye CTDTSCA was obtained via Knoevenagel condensation reaction of the aldehyde **11** and cyanoacetic acid in the presence of piperidine catalyst in 70% yield [26]. The synthetic methods of dye CTCA and DTSCA were similar to but much simpler than that of CTDTSCA. CTCA was obtained by the treatment of 9-(thiophen-2-yl)-9*H*-carbazole with Vilsmeier–Haack reaction and Knoevenagel condensation. DTSCA was obtained by the Knoevenagel condensation reaction of **4** and cyanoacetic acid in presence of piperidine.

3.2. UV–vis absorption and emission spectra

The UV–vis absorption spectra of the organic dyes in THF are shown in Fig. 1. The **CTDTSCA** has an intense absorption spectrum

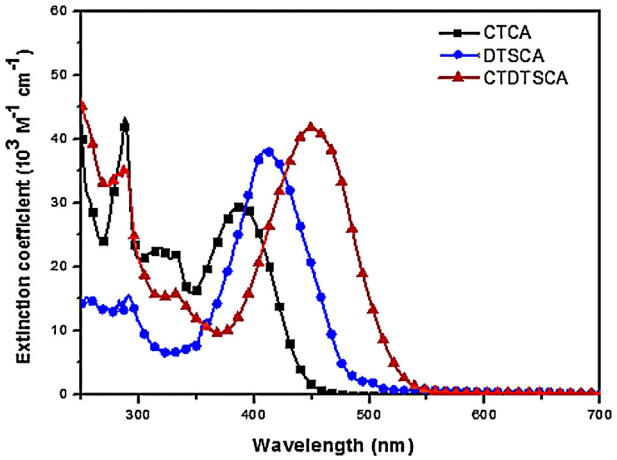

Fig. 1. UV–vis absorption spectra of **CTDTSCA**, **CTCA**, **DTSCA**.

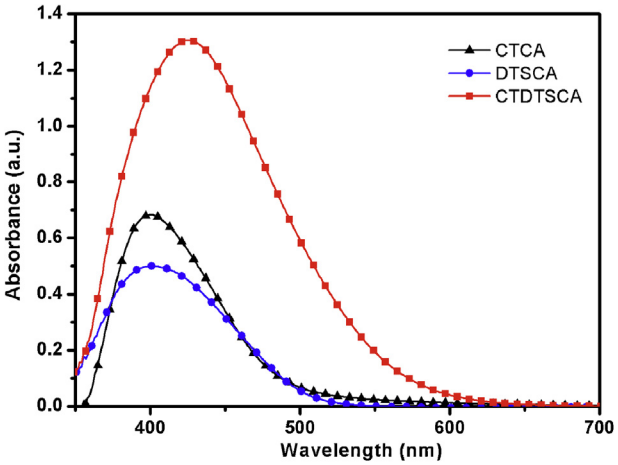

Fig. 3. Absorption spectra of **CTDTSCA**, **CTCA** and **DTSCA** anchoring on the 10 μm porous TiO_2 nanoparticle films.

centerd at 450 nm ($\varepsilon = 4.2 \times 10^4\ M^{-1}\ cm^{-1}$). It shows obvious red-shift in contrast to the maximum absorption wavelength (λ_{max}) of **CTCA** (400 nm) and **DTSCA** (409 nm), demonstrating remarkable effect of **DODTS** unit in narrowing the energy gap and the effective electron-donating function of carbazole unit. The emission spectra of the organic dyes in THF are shown in Fig. 2. The emission band of **CTDTSCA** was centerd at 554 nm when excited on its maximum absorption.

Absorption spectra of **CTDTSCA**, **CTCA** and **DTSCA** anchoring on the 10 μm porous TiO_2 nanoparticle films are shown in Fig. 3, the λ_{max} of **CTDTSCA** exhibits slightly blue-shifted behaviour in comparison with that in THF solution. It may attribute to the weaker electron drawing effect of carboxylate–TiO_2 unit compared to carboxylic acid.

3.3. Electrochemical properties

The first ground-state oxidation potential (***E*ox**), which is corresponding to the **HOMO** level of dye, was measured by cyclic voltammetry (**CV**) with 0.1 M tetrabutylammonium hexafluorophosphate ($TBAPF_6$) in acetonitrile solution, the results are represented in Fig. 4 and Table 1. The **LUMO** levels of sensitizers were calculated by the values of **HOMO** and the zero-zero excitation energy (***E*0–0**), and the latter was estimated from the absorption onset. The energy offset of **LUMO** (−3.14 eV for **CTDTSCA**) with respect to the TiO_2 conduction band edge (−4.00 eV) [27] provides an effective driving force for the electron-injection process. Besides, the **HOMO** level of **CTDTSCA** (−5.14 eV) is lower than the redox potential of I^-/I_3^- couple (−4.60 eV) [28,29], allowing the oxidized sensitizer to accept electrons from I^- to regenerate **CTDTSCA** and avoid the charge recombination between the oxidized dyes and photo-injected electrons in the TiO_2 film. For comparison, the cyclic voltammetry curves of **CTCA** and **DTSCA** were also measured.

As shown in Table 1, **CTDTSCA** possesses a higher **HOMO** level than **DTSCA**, it may be due to effective electron-donating function of carbazole unit and the broadened π conjugation with thiophene-ethynyl-**DODTS**. **DTSCA** shows the lowest **LUMO** level among the three dyes, and **CTDTSCA** has a lower **LUMO** level than **CTCA**, indicating that the incorporation of **DODTS** decrease the **LUMO** level remarkably.

3.4. Theoretical calculations

As replacing the octyl chains linked to silicon with methyl won't make obvious difference in energy or molecular topology of the frontier orbitals [32], the density functional theory (**DFT**) calculations of dimethyl substituted silicon **CTDTSCA**, **CTCA** and **DTSCA** were performed. The isodensity surface plots of **HOMO** and **LUMO** of dimethyl substituted silicon **CTDTSCA**, **CTCA** and **DTSCA** were presented in Fig. 5.

HOMO and LUMO level of dimethyl-substituted **CTDTSCA**, **CTCA** and **DTSCA** calculated by **Guassian 09** are −5.35 eV and −2.90 eV, −5.81 eV and −2.75 eV, −5.71 eV and −2.69 eV, respectively. The

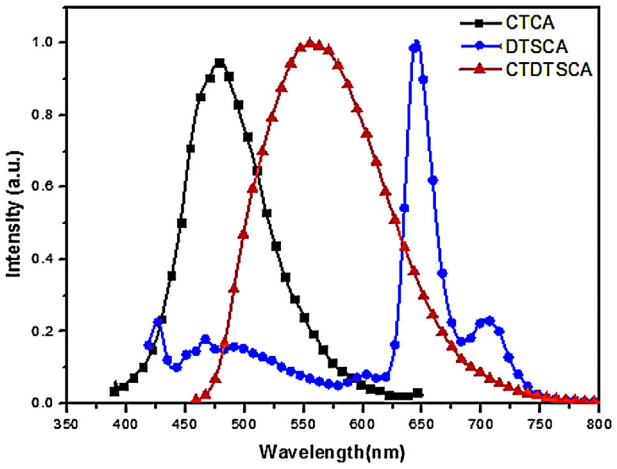

Fig. 2. Emission spectra of **CTDTSCA**, **CTCA**, **DTSCA**.

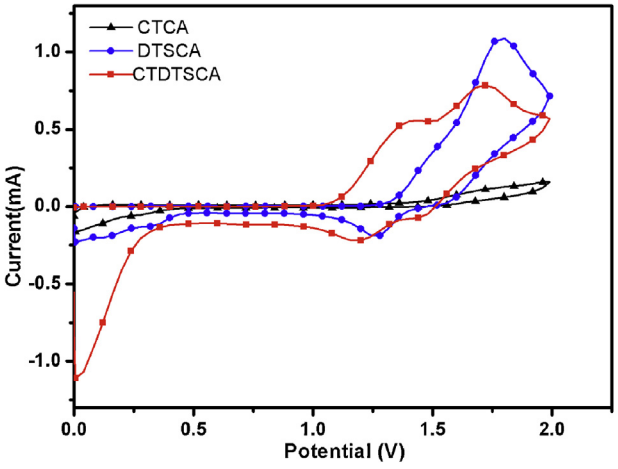

Fig. 4. Cyclic voltammograms of **CTDTSCA**, **CTCA**, and **DTSCA** anchored on TiO_2.

Table 1
Photophysical and electrochemical data for dyes.

Dye	λ_{onset}[a] (nm)	E_g[b] (eV)	$E^{onset}{}_{ox}$ (eV)	E_{HOMO}[c] (eV)	E_{LUMO}[d] (eV)
CTDTSCA	550	2.24	0.98	−5.38	−3.14
CTCA	490	2.53	1.10	−5.50	−2.97
DTSCA	503	2.46	1.35	−5.75	−s3.29

[a] Absorption spectra of dyes on TiO_2 were obtained through measuring the dye adsorbed on TiO_2 nanoparticle film in CH_2Cl_2 solution.
[b] The optical gap E_g was estimated from the onset point of the absorption spectra: $E_g = 1240/\lambda_{onset}$.
[c] The oxidation potentials of dye anchored on TiO_2 were measured with 0.1 M tetrabutylammonium hexaflurophosohate ($TBAPF_6$) as electrolyte, HOMO was estimated from $E_{HOMO} = -(4.4 + E^{onset}{}_{ox})$ eV [30,31].
[d] $E_{LUMO} = E_{HUMO} + E_g$.

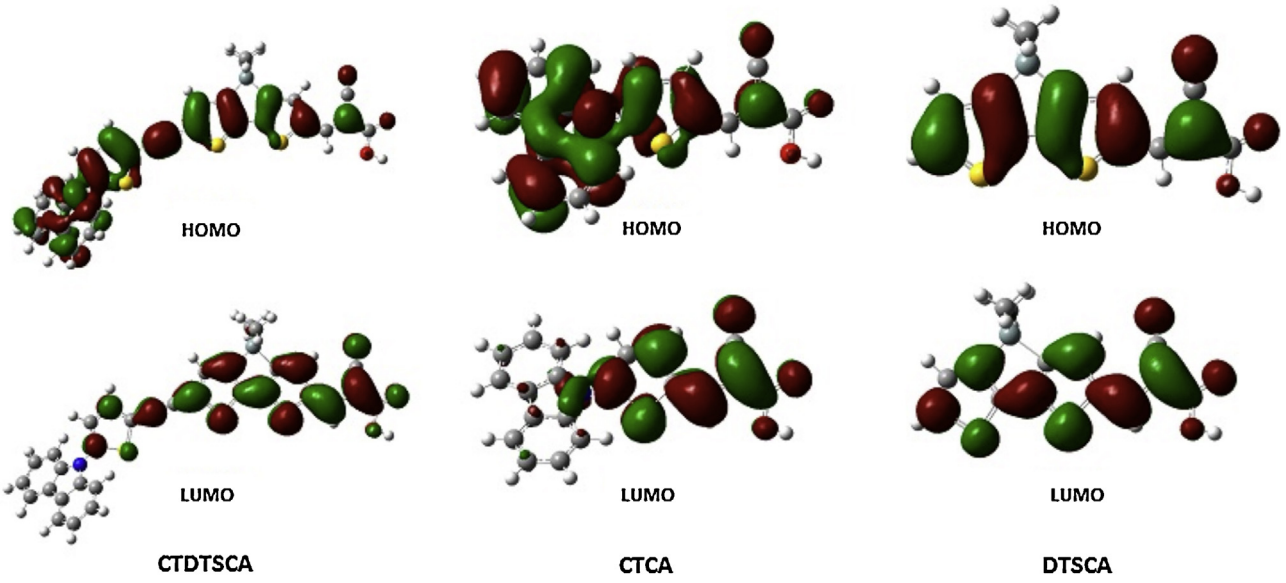

Fig. 5. Frontier molecular orbital of dimetyl-substituted **CTDTSCA**, **CTCA** and **DTSCA**.

energy gaps are 2.45 eV, 3.06 eV, 3.02 eV, respectively. These results are close to the data from **CV**. The slight difference of the theoretical calculations and experimental data can be attributed to the neglect of solvent effect in theory calculation, the tendency of **DFT** to overestimate π-conjugation and the replacement of octyl with methyl [33].

3.5. Photovoltaic performances

The incident monochromatic photon-to-current conversion efficiency (**IPCE**) spectra of **DSSC** sensitized by **CTDTSCA**, **CTCA** and **DTSCA** are shown in Fig. 6. The **IPCE** of **CTDTSCA** exceeds 60% from 364 nm to 500 nm, reaching its maxima of nearly 70%. The **IPCE** spectrum of **CTDTSCA** is higher and greatly wider than that of **CTCA**, as can be expected from the absorption spectra. It may be attributed to good electron-transferring capacity and effective function in narrowing the energy gap of **DODTS** unit. The **IPCE** of **CTCA** exceeds 50% from 370 nm to 510 nm and reaches its peak of nearly 65%, while the **IPCE** of **DTSCA** almost stays below 20%. It implicates that **DODTS** unit plays little role in electron-donating and *N*-substituted carbazole displays strong electron-donating effect in the **CTDTSCA** molecule.

The reason of the improved performance of **CTDTSCA** can also be proved by theoretical calculation (Fig. 5). As shown in Fig. 5, **HOMO** of dimethyl-substituted **CTDTSCA** is delocalized through the whole molecule. **LUMO** of dimethyl-substituted **CTDTSCA** was populated over thiophene, ethynyl, dimethyl-substituted dithienosilole (**DMDTS**) and cyanoacrylic acid fragments with sizable contribution from **DMDTS** and cyanoacrylic acid fragments. This spatially directed separation of **HOMO** and **LUMO** is an ideal condition for

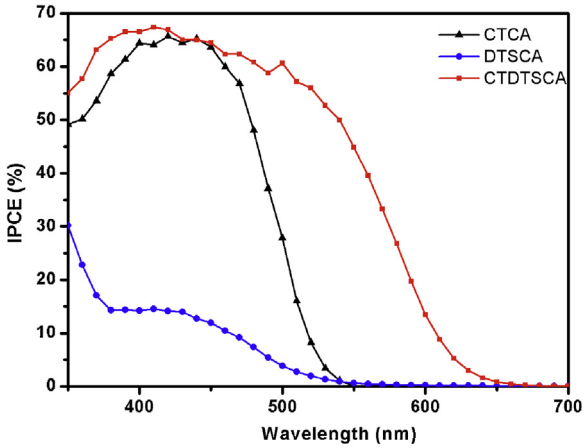

Fig. 6. IPCE spectra of DSSC based on **CTDTSCA**, **CTCA** and **DTSCA**.

dye-sensitized solar cell, which facilitates ultrafast interfacial electron injection from excited dyes to TiO_2.

Additionally, the hole location on the carbazole unit facilities the electron donor to approach, promoting the dye regeneration. Furthermore, **HOMO** and **LUMO** exhibit overlapping extension to the thiophene, ethyne and **DMDTS** spacers, strengthening the electronic coupling parallel to the transition dipole moment between the two electronic states, which in turn increases the strength between the two states. It's worthy to mention that σ^*–π^* hyperconjugation, characteristic of the silole ring, was not inspected from the **LUMO** orbital plot, probably arising from the energetic

Table 2
Photovoltaic performance of DSSC sensitized by CTDTSCA, CTCA, DTSCA[a].

Dye	J_{sc} (mA cm^{-2})	V_{oc} (V)	FF	η (%)
CTDTSCA	10.54	0.68	0.67	4.80
CTCA	6.48	0.62	0.71	2.83
DTSCA	1.64	0.52	0.67	0.57

[a] Under AM 1.5 illumination (power 100 mW cm^{-2}) with an active area of 0.25 cm^2.

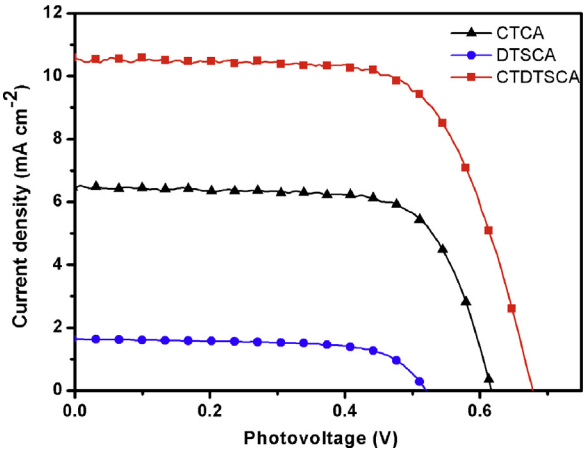

Fig. 7. Photocurrent density vs voltage for DSSC based on **CTDTSCA**, **CTCA** and **DTSCA** under AM 1.5 G simulated solar light (100 mW cm^{-2}).

stabilization of carbon-backbone-based π^*-orbital by the strong electron-withdrawing cyanoacrylic fragment.

The photovoltaic parameters of **DSSC** sensitized by **CTDTSCA**, **CTCA** and **DTSCA** are listed in Table 2. Fig. 7 shows the current density–voltage (*J*–*V*) curves of the **DSSC** sensitized by the above dyes under standard global AM 1.5G solar irradiation. The short-circuit photocurrent density (J_{sc}), open-circuit voltage (V_{oc}), and fill factor (FF) of the solar cell based on **CTDTSCA** are 10.54 mA cm^{-2}, 0.67 V, and 0.67, respectively, yielding an overall power conversion efficiency (η) of 4.80%. Under the same condition, the devices based on **CTCA** and **DTSCA** obtained much lower conversion efficiencies of 2.83% and 0.57%, respectively. These differences in photovoltaic properties were consistent with the **IPCE-λ** spectra, in which the curve of **CTDTSCA** is higher and broader than that of **CTCA** and **DTSCA**. It indicates that the introduction of **DODTS** can effectively improve the performance of dye sensitizer. The poor performance of **DSSC** sensitized by **DTSCA** presumably owed to the lack of rich-electron group, for example, carbazole. **DSSC** sensitized by **CTDTSCA** and **CTCA** both got a medium or higher power conversion efficiency, these results reflect effective electron-donating function of *N*-substituted carbazole.

The electrochemical impedance spectroscopy (**EIS**) was carried on in the dark. The **EIS** analysis provides information about interfacial charge transfer process. Fig. 8 shows the typical Nyquist plots of both electrodes at an applied bias of −0.70 V. In both cells, a larger semicircle occurs in the lower frequency range and a smaller semicircle occurs in the higher frequency range. The larger semicircle corresponds to the charge-transfer process at the TiO_2/dye/electrolyte interface, while the smaller semicircle corresponds to the charge-transfer process at the Pt/electrolyte interface. The difference in smaller semicircles at higher frequencies is small, but the difference in larger semicircles is significant. The much larger radii of the lower frequency semicircles of the **CTDTSCA** cell indicates a stronger charge-transfer resistance at the TiO_2/dye/electrolyte interface.

Fig. 9 shows the **EIS** Bode plots of the **DSSC** based on **CTDTSCA** and **CTCA**. The peak feature at higher frequency corresponds to

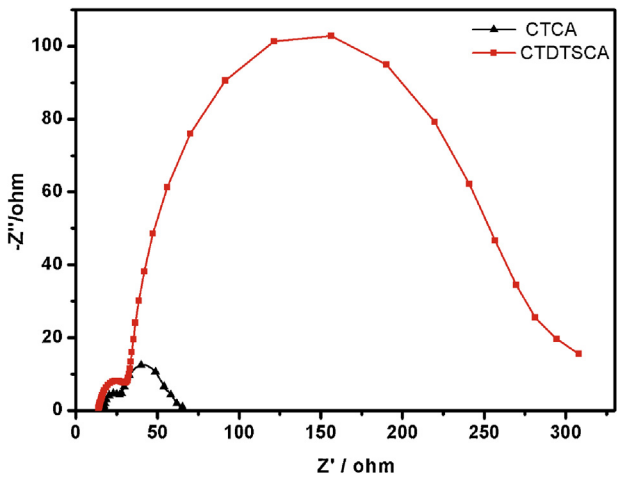

Fig. 8. EIS Nyquist plots (i.e., minus imaginary part of the impedance $-Z''$ vs the real part of the impedance Z' when sweeping the frequency) for DSSC based on **CTDTSCA** and **CTCA** dyes.

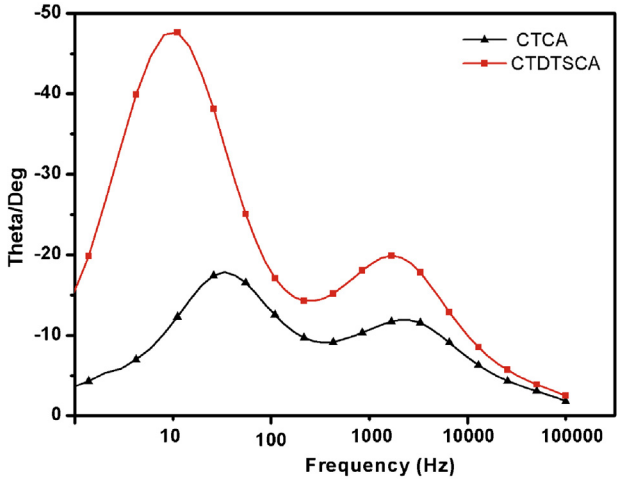

Fig. 9. EIS Bode plots (i.e., the phase of the impedance vs the frequency) for DSSC based on **CTDTSCA** and **CTCA** dyes.

the charge transfer at the Pt/electrolyte interface and the one at lower frequency corresponds to the charge-transfer process at the TiO_2/dye/electrolyte interface. The characteristic frequency of the lower frequency peak in the Bode plot is related to the charge recombination rate, and its reciprocal is associated with the electron lifetime [34,35]. The lower frequency peak of the **CTDTSCA** cell shifts to a lower frequency compared to the **CTCA** cell, indicating less charge recombination and longer electron lifetime at the TiO_2/dye/electrolyte interface. Both the EIS Nyquist and Bode plots suggest that the insert of **DODTS** unit in the dye molecule greatly improves the charge-transfer ability at the TiO_2/dye/electrolyte interface. We deduce that the long octyl chains may partly act as the blocking units between TiO_2 surface and electrolyte, preventing I_3^- ions approaching the TiO_2 surface.

4. Conclusion

To summarize, we had successfully synthesized a novel **D–π-A** pattern organic dye sensitizer **CTDTSCA**, in which dithienosilole unit acted as π-conjugated system**,** carbazole moiety acted as electron donor, and cyanoacrylic acid unit acted as electron acceptor. The **DSSC** sensitized by it reached a medium-high power conversion efficiency of 4.80%. It indicated that the dye with *N*-substituted

carbazole utilized as the electron donor can obtain promising photoelectric property. **CTDTSCA** possesses larger absorption maxima and narrower energy gap than that of **CTCA** (in which thiophene acted as π-conjugated system), leading to **DSSC** sensitized by **CTDTSCA** possesses better photovoltaic performances than **DSSC** sensitized by **CTCA**. It may be attributed to the incorporation of **DODTS** unit, which can broaden the π-conjugation and effectively reduce the LUMO level. These results revealed the potential value of **DODTS** unit in designing ideal organic dye sensitizer.

Acknowledgements

The authors are grateful to financial support from the National Natural Science Foundation of China (No. 20872035, 21076078), Hangzhou Normal University, and the East China University of Science and Technology.

Appendix A. Supplementary data

Supplementary data associated with this article can be found, in the online version, at http://dx.doi.org/10.1016/j.jphotochem.2014.07.021.

References

[1] R. Faccio, W.L. Fernández, H. Pardo, A.W. Mombrú, Recent Pat. Nanotechnol. 5 (2011) 46–62.
[2] (a) S. Ito, S.M. Zakeeruddin, B.R. Humphry, P. Liska, R. Charvet, P. Comte, M.K. Nazeeruddin, P. Pechy, M. Takata, H. Miura, S. Uchida, M. Grätzel, Adv. Mater. 18 (2006) 1202–1205;
(b) S. Ito, H. Miura, S. Uchida, M. Takata, K. Sumioka, P. Liska, P. Comte, P. Pechy, M. Grätzel, Chem. Commun. 41 (2008) 5194–5196;
(c) G. Zhang, H. Bala, Y. Cheng, D. Shi, X. Lv, Q. Yu, P. Wang, Chem. Commun. 16 (2009) 2198–2200;
(d) H. Im, S. Kim, C. Park, S.H. Jang, C.J. Kim, K. Kim, N.G. Park, C. Kim, Chem. Commun. 46 (2010) 1335–1337.
[3] W. Zeng, Y. Cao, Y. Bai, Y. Wang, Y. Shi, M. Zhang, F. Wang, C. Pan, P. Wang, Chem. Mater. 22 (2010) 1915–1925.
[4] (a) S.G. Awuah, J. Polreis, J. Prakash, Q.Q. Qiao, Y.J. You, J. Photochem. Photobiol. A 224 (2011) 116–122;
(b) W.Y. Wong, G.J. Zhou, X.M. Yu, H.S. Kwok, B.Z. Tang, Adv. Funct. Mater. 16 (2006) 838–846;
(c) G. Zhou, W.Y. Wong, B. Yao, Z. Xie, L. Wang, Angew. Chem. Int. Ed. 46 (2007) 1149–1151.
[5] R. Tarsang, V. Promarak, T. Sudyoadsuk, S. Namuangruk, S. Jungsuttiwong, J. Photochem. Photobiol. A 273 (2014) 8–16.
[6] Y. Ooyama, Y. Shimada, A. Ishii, G. Ito, Y. Kagawa, I. Imae, K. Komaguchi, Y. Harima, J. Photochem. Photobiol. A 203 (2009) 177–185.
[7] A.C. Onicha, K. Panthi, T.H. Kinstle, F.N. Castellano, J. Photochem. Photobiol. A 223 (2011) 57–64.
[8] Z.S. Wang, N. Koumura, Y. Cui, M. Takahashi, H. Sekiguchi, A. Mori, T. Kubo, A. Furube, K. Hara, Chem. Mater. 20 (2008) 3993–4003.
[9] N. Koumura, Z.S. Wang, S. Mori, M. Miyashita, E. Suzuki, K.A. Hara, J. Am. Chem. Soc. 128 (2006) 14256–14257.
[10] (a) Q.Q. Li, L.L. Lu, C. Zhong, J. Shi, Q. Huang, X.B. Jin, T.Y. Peng, J.G. Qin, Z. Li, J. Phys. Chem. B 113 (2009) 14588–14595;
(b) Q.Q. Li, L.L. Lu, C. Zhong, J. Huang, Q. Huang, J. Shi, X.B. Jin, T.Y. Peng, J.G. Qin, Z. Li, Chem. Eur. J. 15 (2009) 9664–9668.
[11] V. Jeux, D. Demeter, P. Leriche, J. Roncali, RSC Adv. 3 (2013) 5811–5814.
[12] (a) A.J. Qin, J.W.Y. Lam, B.Z. Tang, Prog. Polym. Sci. 37 (2012) 182–209;
(b) S.C. Yin, J. Zhang, H.K. Feng, Z.J. Zhao, L.W. Xu, H.Y. Qiu, B.Z. Tang, Dyes Pigments 95 (2012) 174–179;
(c) W.F. Shu, C.W. Guan, W.H. Guo, C.Y. Wang, Y.J. Shen, J. Mater. Chem. 22 (2012) 3075–3081;
(d) J. Liu, C.X. Yan, S.S. Li, C.Y. Wang, Y.J. Shen, Chin. J. Chem. 30 (2012) 2861–2868.
[13] K.H. Lee, J. Ohshita, A. Kunai, Organometallics 23 (2004) 5481–5487.
[14] J. Ohshita, M. Nodono, T. Watanabe, Y. Ueno, A. Kunai, Y. Harima, K. Yamashita, J. Organomet. Chem. 553 (1998) 487–491.
[15] D. Enders, R. Pieter, B. Renger, D. Seebach, Org. Synth. 6 (1988) 542.
[16] N. Miyaura, A. Suzuki, Org. Synth. 8 (1993) 532.
[17] M.J. Frisch, G.W. Trucks, H.B. Schlegel, G.E. Scuseria, M.A. Robb, J.R. Cheeseman, G. Scalmani, V. Barone, B. Mennucci, G.A. Petersson, H. Nakatsuji, M. Caricato, X. Li, H.P. Hratchian, A.F. Izmaylov, J. Bloino, G. Zheng, J.L. Sonnenberg, M. Hada, M. Ehara, K. Toyota, R. Fukuda, J. Hasegawa, M. Ishida, T. Nakajima, Y. Honda, O. Kitao, H. Nakai, T. Vreven, J.A. Montgomery Jr., J.E. Peralta, F. Ogliaro, M. Bearpark, J.J. Heyd, E. Brothers, K.N. Kudin, V.N. Staroverov, R. Kobayashi, J. Normand, K. Raghavachari, A. Rendell, J.C. Burant, S.S. Iyengar, J. Tomasi, M. Cossi, N. Rega, J.M. Millam, M. Klene, J.E. Knox, J.B. Cross, V. Bakken, C. Adamo, J. Jaramillo, R. Gomperts, R.E. Stratmann, O. Yazyev, A.J. Austin, R. Cammi, C. Pomelli, J.W. Ochterski, R.L. Martin, K. Morokuma, V.G. Zakrzewski, G.A. Voth, P. Salvador, J.J. Dannenberg, S. Dapprich, A.D. Daniels, O. Farkas, J.B. Foresman, J.V. Ortiz, J. Cioslowski, D.J. Fox, Gaussian 09, Revision A. 01, Gaussian, Inc., Wallingford, CT, 2009.
[18] S. Mishra, A. Palai, R. Srivastava, M. Kamalasanan, M. Patr, J. Polym. Sci., A: Polym. Chem. 47 (2009) 6514–6525.
[19] G. Lu, H. Usta, C. Risko, L. Wang, A. Facchetti, M.A. Ratner, T.J. Marks, J. Am. Chem. Soc. 130 (2008) 7670–7685.
[20] L.Y. Lin, C.H. Tsai, K.T. Wong, T.W. Huang, L. Hsieh, S.H. Liu, H.W. Lin, C.C. Wu, S.H. Chou, S.H. Chen, A. Tsa, J. Org. Chem. 75 (2010) 4778–4785.
[21] P.M. Beaujuge, W. Pisula, H.K. Tsao, S. Ellinger, K. Müllen, J.R. Reynolds, J. Am. Chem. Soc. 131 (2009) 7514–7515.
[22] R.H. Mitchell, Y.H. Lai, R.V. Williams, J. Org. Chem. 44 (1979) 4733–4735.
[23] Q. Zhang, J.S. Chen, Y.X. Cheng, L.X. Wang, D.G. Ma, X.B. Jing, F.S. Wang, Mater. Chem. 14 (2004) 895–900.
[24] R.A. Batey, M. Shen, A.J. Lough, Org. Lett. 4 (2002) 1411–1414.
[25] A.O. King, N. Yasuda, Organomet. Chem. 6 (2004) 205–245.
[26] K. Do, D. Kim, N. Cho, S. Paek, K. Song, J. Ko, Org. Lett. 14 (2012) 222–225.
[27] G. Zhang, Y. Bai, R. Li, D. Shi, S. Wenger, S.M. Zakeeruddin, M. Grätzel, P. Wang, Energy Environ. Sci. 2 (2009) 92–95.
[28] A. Hagfeldf, M. Grätzel, Chem. Rev. 95 (1995) 49–68.
[29] M. Grätzel, Nature 414 (2001) 338–344.
[30] A.K. Agrawal, S.A. Jenekhe, Chem. Mater. 8 (1996) 579–589.
[31] Y.F. Li, Y. Cao, J. Gao, D.L. Wang, G. Yu, A.J. Heeger, Synth. Met. 99 (1999) 243–248.
[32] H. Huang, J. Youn, R.P. Ortiz, Y. Zheng, A. Facchetti, T. Marks, Chem. Mater. 23 (2011) 2185–2200.
[33] J.R. Reimers, Z.L. Cai, A. Bilic, N.S. Hush, Ann. N.Y. Acad. Sci. 1006 (2003) 235–251.
[34] M. Adachi, M. Sakamoto, J. Jiu, Y. Ogata, S. Isoda, J. Phys. Chem. B 110 (2006) 13872–13880.
[35] Q. Wang, J. Moser, M. Grätzel, J. Phys. Chem. B 109 (2005) 14945–14953.